AIMS Materials Science, 13(5): 967–975.
DOI: 10.3934/matersci.2026045
Received: 29 August 2026
Revised: 12 October 2026
Accepted: 26 October 2026
Published: 30 October 2026

https://www.aimspress.com/journal/Materials

Research article

Nitrogen-doped carbon with three-dimensional interconnected wrinkled lamellar hierarchical porous framework for high-performance aqueous Zn-I_2 batteries

Xianhe Meng[1,2,*], Qi Shen[2], Aobo Yue[2], Tao Chen[3] and Zonghua Wang[1,*]

[1] College of Chemistry and Chemical Engineering, Qingdao University, Qingdao 266071, China
[2] College of Materials and Chemistry, China Jiliang University, Hangzhou 310018, China
[3] Shaoxing Electric Power Equipment Co., Ltd. Shaoxing 312000, China

* **Correspondence:** Email: mengxhe@cjlu.edu.cn, wangzonghua@qdu.edu.cn; Tel: +86-0571-86835740, +86-0532-85951196.

Supplementary

1. Experimental section

1.1. Reagents

All chemical reagents were used as received without further purification: zinc nitrate hexahydrate (Macklin, ≥99%), N,N-dimethylformamide (DMF) (Aladdin, AR), 2-methylimidazole (Aladdin, 98%), triethylamine (Wuxi Prospec Chemical Reagent Co., Ltd., AR), anhydrous methanol (Macklin, ≥99.5%), anhydrous ethanol (Hangzhou Gaojing Chemical Co., Ltd., AR), potassium citrate (Macklin, ≥98%), iodine (I_2) (Aladdin, 99.99%), conductive carbon black (TIMCAL, Super P), zinc sulfate heptahydrate (Aladdin, AR), polytetrafluoroethylene (PTFE) (Macklin, <1 μm).

1.2. Synthesis of ZIF-8-gel

A gel-based method was employed for the synthesis of ZIF-8-gel crystals. Solution A was prepared by dissolving 0.893 g of zinc nitrate hexahydrate in 3 mL of DMF via sonication. Solution B was obtained by dissolving 0.985 g of 2-methylimidazole in 3 mL of DMF, followed by the addition of 1.214 g of triethylamine. Solutions A and B were mixed under stirring, sonicated for 5 s, and allowed to equilibrate to form a homogeneous super ZIF-8 gel. After DMF immersion, centrifugation and repeated DMF/methanol washing, ZIF-8-gel underwent sequential drying at 60 °C (air, overnight) and 110 °C (vacuum, 12 h).

1.3. Electrode and battery fabrication

Iodine loading was achieved by mixing 0.1 g of carbon material with 1.0 g of I_2 (99.99%) in a sealed vial at 120 °C for 2 h, followed by desorption at 80 °C for 2 h. Iodine adsorption capacities were 66.5% (C-Z), 68.2% (C-K), and 70.1% (C-Z-K), respectively. The electrodes were prepared by mixing active carbon materials (C-Z, C-K, C-Z-K), conductive Super P carbon black, and PTFE aqueous solution (10 wt.%) in a mass ratio of 7:1.5:1.5. The slurry was ground, pressed into uniform sheets, vacuum-dried at 40 °C for 12 h, and punched into 12 mm diameter disks. Coin cells (LIR2025) were assembled using the iodine-loaded carbon material as the cathode (with an active material loading of 1.87 mg cm^{-2}), zinc foil as the anode, Whatman GF/A glass fiber as the separator, and 2.0 mol L^{-1} $ZnSO_4$ aqueous solution as the electrolyte. In the electrochemical performance tests, 1 C was defined as 170 mAh g^{-1}.

1.4. Characterization

The X-ray diffraction (XRD) patterns were obtained on a Bruker D8 Advance diffractometer with a Cu-Kα target (wavelength = 1.54056 Å). Raman spectroscopy (LabRamHR800, 532 nm laser) was used to investigate the samples. The microscopic morphology was observed using field-emission scanning electron microscopy (JSM-6700, JEOL/Japan) equipped with an energy-dispersive X-ray spectroscopy (EDS) instrument. The porosity and specific surface area of the carbon samples was characterized by using the ASAP 2420 (Micromeritics) equipped with the micropore option.

Cyclic voltammetry (CV) was tested using an electrochemical workstation (CHI660E, Shanghai CH Instrument Co., Ltd.). The potential range was from 0.6 to 1.6 V. The constant current charge-

discharge tests were all conducted on the battery testing system (CT200IA, Wuhan Land Electronics Co., Ltd.). The potential range was 0.6 to 1.6 V, and the nominal specific capacity of the zinc-iodine battery was 211 mAh g^{-1}.

2. Supplementary Figures

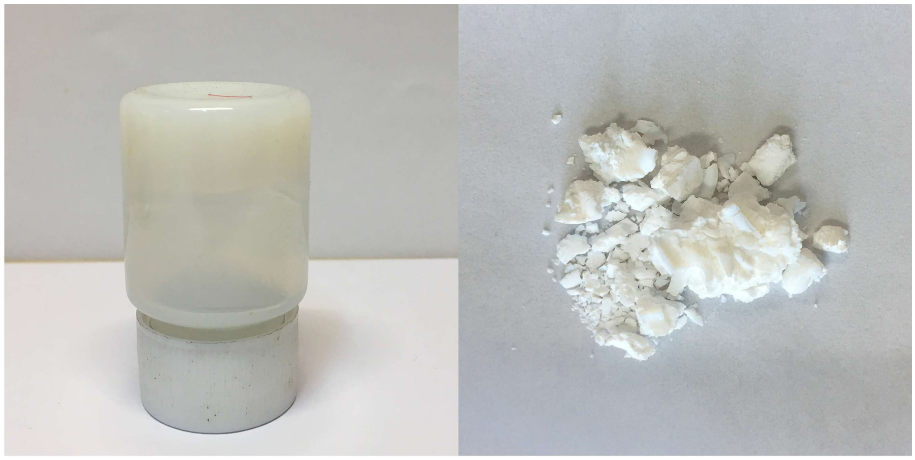


Figure S1. The photo of ZIF-8-gel before and after drying.

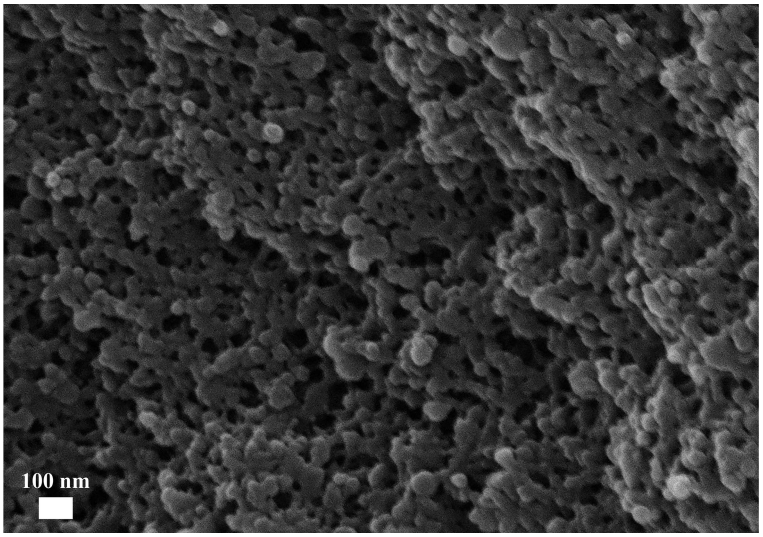


Figure S2. The SEM images of ZIF-8-gel.

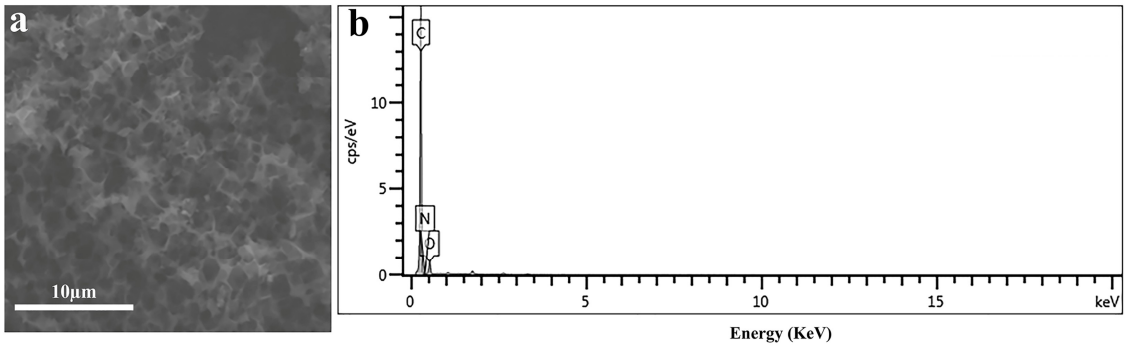


Figure S3. (a) Scanning electron microscope energy spectrum selection image and (b) elemental content maps of C-Z-K materials (C: 88.94 wt.%; N: 0.96 wt.%; O: 10.10 wt.%).

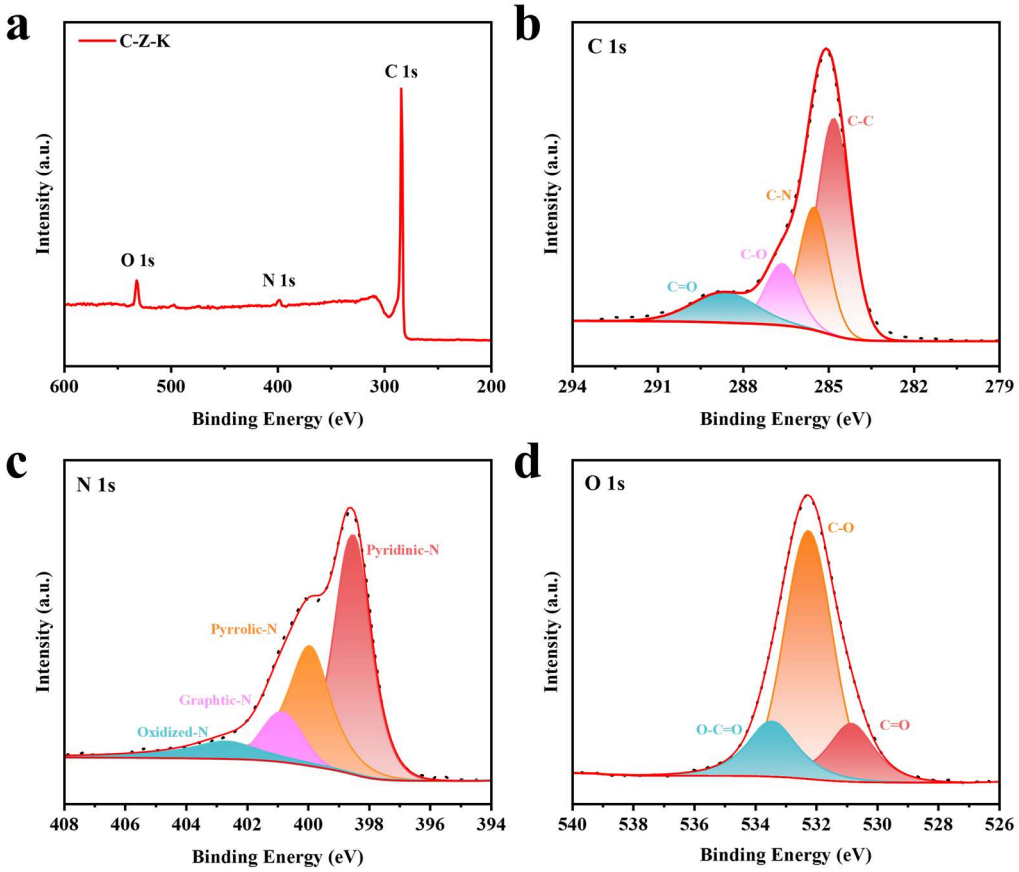


Figure S4. XPS spectra of the C-Z-K material: (a) survey spectrum; (b) C 1s; (c) N 1s; (d) O 1s.

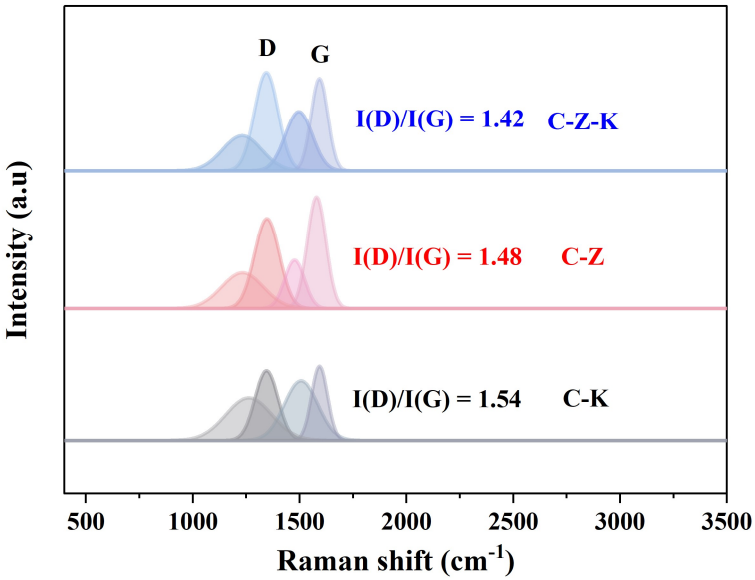


Figure S5. Lorentz curve fitting of Raman spectra for C-K, C-Z and C-Z-K.

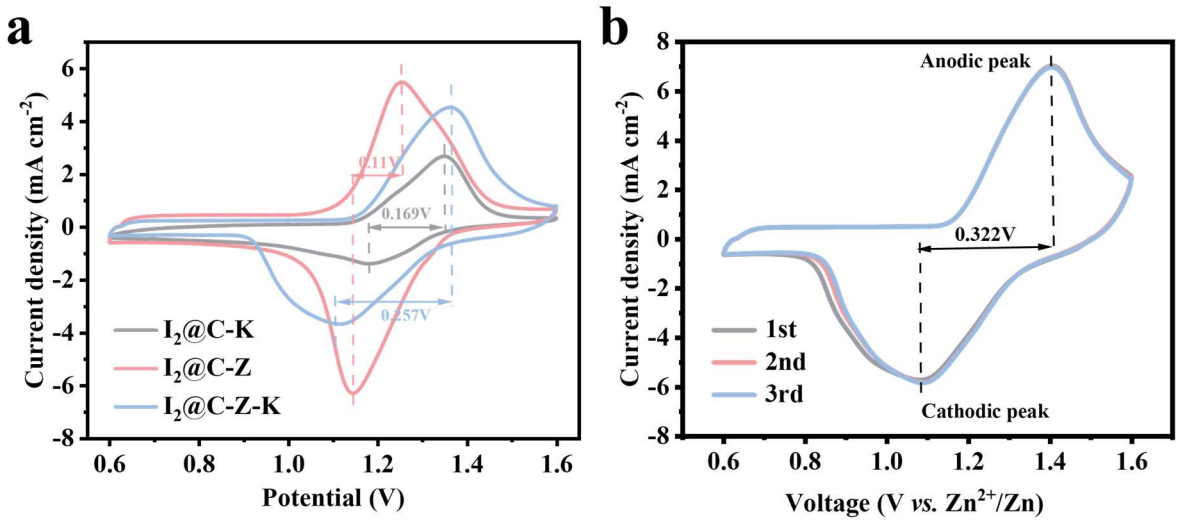


Figure S6. (a) CV curves of I_2@C-Z-K, I_2@C-Z and I_2@C-K tested at 1 mV s^{-1}. (b) CV curves of the first three cycles for I_2@C-Z-K.

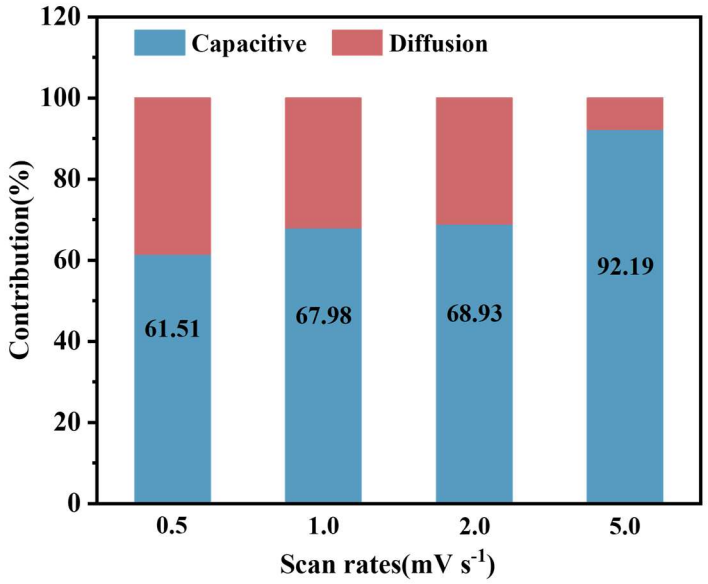


Figure S7. Pseudocapacitive contribution ratios of I_2@C-Z-K at different scan rates.

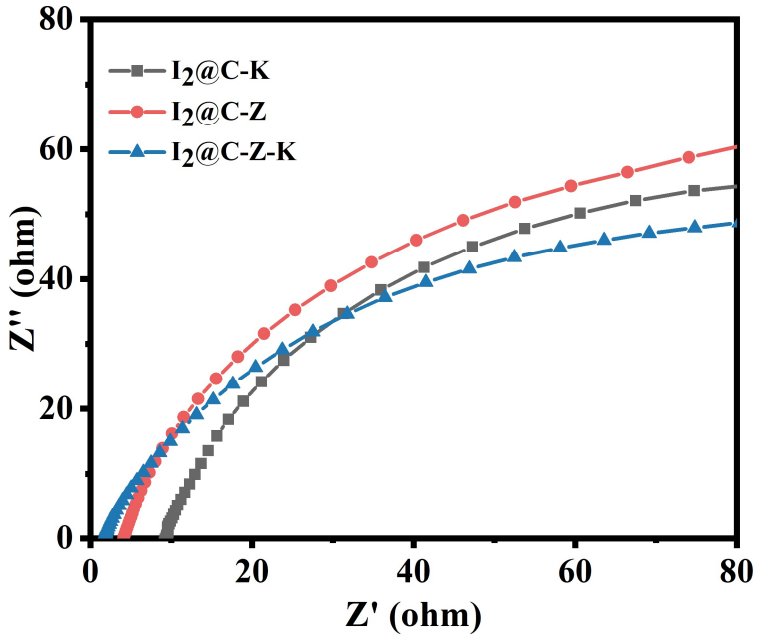


Figure S8. The Nyquist plots of the Zn/C-I_2 batteries in the initial state before cycling.

AIMS Press

© 2026 the Author(s), licensee AIMS Press. This is an open access article distributed under the terms of the Creative Commons Attribution License (https://creativecommons.org/licenses/by/4.0)